

Advanced Modeling of CSP Plants with Sensible Heat Storage: Instantaneous Effects of Solar Irradiance

Behnam Mostajeran Goortani*[‡], Hossein Heidari**

* Renewable Energy Engineering Department, Faculty of Advanced Sciences and Technologies, University of Isfahan, Iran,

** Renewable Energy Engineering Department, Faculty of Advanced Sciences and Technologies, University of Isfahan, Iran,
(b.mostajeran@ast.ui.ac.ir, heidarividooji@yahoo.com)

[‡] Corresponding Author; First Author, Postal address, Tel: +98 9103450496, Fax: +98 31 37934229, b.mostajeran@ast.ui.ac.ir

Received: 19.12.2016 Accepted: 14.03.2017

Abstract- A flexible model for concentrated solar thermal power plants with two tank active direct storage system is developed on gPROMS platform. Eutectic mixture of potassium and sodium nitrates salt melt is used as heat transfer fluid and storage medium. The solar radiation data obtained from a weather station, during 10 years in the city of Isfahan are used. It is showed that the Bird's clear sky model well represents the normalized weather data. The storage system is designed to feed the boiler for 15 hours in the absence of sun. The model predicts the instantaneous effects of solar irradiance change and calculates variable with time parameters of the CSP plant; namely, the salt melt flow rates through receiver and boiler, and tank levels during 24 hr. The results indicate that a collector surface area of 35 m² and 250Kg mixture of nitrate salts, per 1 KW electricity generation, is necessary. Respecting the "variable with time" nature of solar irradiance, the role of storage tanks to damp fluctuations in process parameters of a CSP plant is further quantified. A 2500 Kg of heat storage material eliminates the need to variable collector surface area 100 m² to 1500 m² or equivalently, eliminated too high boiler temperatures (1000 °C).

Keywords The Bird's model, thermal energy storage, salt melt, solar irradiance, concentrated solar power.

1. Introduction

Two methods are used to harvest sun energy; methods based on using photovoltaic cells and the ones based on using thermal collectors. In both methods, it is important to respect the variable with time nature of solar irradiance. The effects of weather conditions and changes in solar irradiance on the performance of PV pilot plants is studied parametrically [1]. In concentrated solar thermal collectors the variable with time nature of solar irradiance plays an important role, because collector performance depends on the direct component of solar irradiance. Therefore suitable comprehensive models are desirable to be able to parametrically study CSP plants and to model the dynamics of the process [2].

There are two thermodynamic cycles exchanging energy in a CSP plant, solar thermal energy collection and storage, and power plant cycles. In the solar heat collection cycle, solar radiation energy is received to increase the temperature of the heat transfer medium. In the literature, to model solar irradiance, the Bird's clear sky model has attracted much attention. It considers the effects of absorption of different

gases and the moisture in the atmosphere. Other models as the Hottel's are also developed [6].

Various mechanisms for the thermal heat storage are proposed, direct, indirect, active, passive, single tank or dual tank systems [4]. The storage medium is usually heat transfer oil, for low to medium temperature, and salt melts for the high temperature storage. Molten metals are applied because of heat high heat transfer rates [13]. For CSP plants, higher temperatures are desirable; therefore, salt melts have attracted more attention. For economic issues, solid low cost materials like cement or sand are applied [15].

In the power plant cycle, Rankine cycle with reheat and fresh water preheating is mostly used in the today's power plants, including CSP plants [8,9].

gPROMS is advanced modeling software used to model mass and energy balances over equipment and processes under dynamic or steady state conditions. However, the software is mainly used in the oil and gas research sector so far [3]. Along with Multiflash and material properties data banks, this modeling software allows the model developer to write suitable equations of mass and energy balances and

simultaneously solve the equations assuming variable physical and thermodynamic properties of materials. These properties in vapor and liquid phases, are written as functions of pressure, temperature, and components fractions.

Different softwares are used in the literature to simulate power plants [10,12,14]; however, the libraries are of limited use and developments of suitable sub models of the whole CSP plant are time consuming. The objective of the current work is to develop a comprehensive model purely on gPROMS to study the instantaneous effects of solar irradiance changes on the three fundamental components of a CSP plant; namely: heat collection, thermal storage, and power plant. With respect to the “variable with time” nature of solar irradiance, the role of storage tanks to damp fluctuations in process parameters of a CSP plant is further quantified. A 2500 Kg of heat storage material eliminates variable collector surface area need of 100 m² to 1500 m² or equivalently, eliminated the need to increase boiler temperature of greater than 1000 °C.

2. CSP Plant Modelling

2.1. Solar irradiance and collector model

Solar irradiance and collection model is composed of two sets of equations, the collector model and the solar irradiance model. The collector provides the heat required in the generator according to:

$$Q = \text{Area} \cdot \eta \cdot I_{\text{avg}} \tag{1}$$

$$I_{\text{avg}} = \int I_b dt \tag{2}$$

Where, η is the overall thermal collector efficiency and I_{avg} is the average sun radiation intensity during a day. I_{avg} is calculated from the Bird’s model [5]. A collector and receiver overall efficiency of 80% is considered. The overall efficiency depends on the mirrors reflectivity, cleanness, receiver absorption [11]. This model considers the effects of environmental factors and calculates the instantaneous intensity of sun thermal energy. The radiation intensity according to this model is:

$$I_b = 0.9662 \cdot I_0 \cdot \cos(\theta_z) \cdot T_R \cdot T_o \cdot T_{UM} \cdot T_W \cdot T_A \tag{3}$$

where, T_R , T_o , T_{UM} , T_W , and T_A are respectively Rayleigh diffraction, ozone absorption, gas mixtures absorption (O₂ and CO₂), water absorption, and fine particles diffraction. I_0 is the radiation received outside the earth atmosphere and θ_z is the zenith angle.

Parameter I_0 depends on geographic location, time of the day, and date according to the following equation [5]:

$$I_0 = I_{sc} \cdot [1 + 0.034 \cdot \cos(360 \cdot N \cdot r / 365.25)] \tag{4}$$

where, I_{sc} is solar constant (1367 w/m²), N is number of the day from January first and, r considers the effect of geographic location and solar time according to the implicit equation:

$$\cos(z \cdot r) = \sin(\delta \cdot r) \cdot \sin(\phi \cdot r) + \cos(\delta \cdot r) \cdot \cos(\omega \cdot r) \cdot \cos(\phi \cdot r) \tag{5}$$

where, ϕ , δ , and ω , are azimuth, date, and solar time, respectively:

$$\delta = 23.45 \cdot \sin(0.0172 \cdot (284 + N)) \tag{6}$$

$$\omega = 15 \cdot (t_s - 12) \tag{7}$$

where, t_s is solar time.

All the above equations are written in gPROMS and the resultant model calculates the required collector area and radiation intensity. The model inputs are date, time, and geographic location.

2.2. Power plant model

The power plant, a Rankine cycle, is composed of boiler, condensing turbine, total condenser, pump I, fresh water heater (FWH), and pump II according to Fig. 1. Water is used as the working fluid.

Mass and energy balances are written and simultaneously solved in gPROMS. While the physical and thermodynamic properties of the liquid and vapor phase are calculated by calling Multiflash file. Multiflash is physical and thermodynamic property calculation software. A Multiflash file with water as the only component is constructed and different thermodynamic and physical property models are set. All liquid and vapor properties such as enthalpy, specific volume, and heat capacities are assumed to be functions of temperature and pressure. In all equations, the indices 1 to 7 refer to different points of the power plant shown in Fig.1.

The pumps’ work is calculated from:

$$w_{s-pump1} = v_1(P_2 - P_1) \tag{8}$$

$$\eta_{s-pump1} = w_{s-pump1} / W_{pump1} \tag{9}$$

$$h_2 = h_1 + w_{pump1} \tag{10}$$

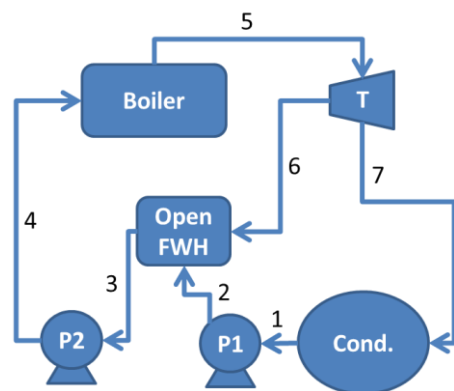


Fig. 1. Schematic of power plant with reheat and fresh water preheating, modeled in gPROMS

where v_1 is specific volume of water, $w_{s-pump1}$ and w_{pump1} are, respectively, isentropic pump work and real pump work (per unit mass of water). h_1 and h_2 and P_1 and P_2 are, respectively, the enthalpies of water and the pressures at points 1 and 2. Similarly for the second pump we have the following equations:

$$W_{s-pump2} = v_1(P_4 - P_3) \tag{11}$$

$$w_{pump2} = W_{s-pump2} / \eta_{s-pump2} \tag{12}$$

$$h_4 = h_3 + w_{pump2} \tag{13}$$

$$P_4 = P_5 \tag{14}$$

Boiler and condenser duties, Q_{boiler} and $Q_{condenser}$ are calculated from:

$$Q_{boiler} = \dot{m}(h_5 - h_4) \tag{15}$$

$$Q_{condenser} = \dot{m}(h_7 - h_1) \tag{16}$$

where \dot{m} is the mass flow rate of water and h_5 , h_4 , h_1 , and h_7 are enthalpies of water at the outlet and inlet of boiler and condenser, respectively. The turbine isentropic efficiency

$\eta_{s-turbine}$ is:

$$\eta_{s-turbine} = w_{turbine} / W_{s-turbine} = (h_5 - h_6) / (h_5 - h_{6s}) \tag{17}$$

$$\eta_{s-turbine} = W_{turbine} / W_{s-turbine} = (h_5 - h_7) / (h_5 - h_{7s}) \tag{18}$$

For the open fresh water heater, FWH, the following equations are used:

$$P_2 = P_3 = P_6 \tag{19}$$

$$yh_6 + (1-y)h_2 = h_3 \tag{20}$$

$$P_7 = P_1 \tag{21}$$

where, y is the mass fraction of turbine vapors that enter the FWH. The total pumps' and turbine's works are:

$$W_{pump1} = (1-y)\dot{m}w_{pump1} \tag{22}$$

$$W_{pump2} = \dot{m}w_{pump2} \tag{23}$$

$$W_{turbine} = \dot{m}[h_5 - yh_6 - (1-y)h_7] \tag{24}$$

Finally the thermal efficiency of the power plant is:

$$\eta_{thermal} = (W_{turbine} - W_{pump1} - W_{pump2}) / Q_{boiler} \tag{25}$$

The above set of equations is simultaneously solved in gPROMS with parameters specified in Table 2. The model results were verified to satisfy the total energy balance of the cycle. Furthermore, to be sure about the accuracy of the models and the correlations used for the calculation of the physical properties, the results were compared with the results of several examples in reference [8] and the agreements between the results were perfect.

Table 1. Transient equations of mass and energy balances for the solar heat collection storage model

$\dot{m}_{boiler} - \dot{m}_{collector} = dM_{cold}/dt$
$\dot{m}_{collector} - \dot{m}_{boiler} = dM_{hot}/dt$
$\frac{d(M_{hot} * T_{hot})}{dt} = \dot{m}_{collector} * T_{out_collector} - \dot{m}_{boiler} * T_{hot}$
$\frac{d(M_{cold} * T_{cold})}{dt} = \dot{m}_{boiler} * T_{boiler} - \dot{m}_{collector} * T_{cold}$
$\int_{t_{sunrise}+1}^{t_{sunset}-1} I_b * \eta * Area * Q_{boiler} dt = 24 * 3600 * Q_{boiler}$
$\dot{m}_{collec} * c_p * (T_{collec} - T_{cold}) = I_b * \eta * Area$
$w_{sunset} = \text{Acos}(-\tan(r * \delta) * \tan(r * \phi)) / r$
$t_{sunset} = 12 + w_{sunset} / 15, t_{sunrise} = 12 - w_{sunset} / 15$
$M_{cold} + M_{hot} = \dot{m}_{boiler} * (t_{sunrise} - t_{sunset} - 2) * 3600$

2.3. Two tank direct storage system model

The heat storage system is composed of two hot and cold tanks, a consumer (boiler), and collector receiver according to Fig. 2. Salt melt from the cold tank is heated in the collector receiver at T_{collec} and is sent and stored in the hot tank. The hot salt melt is then sent to the boiler, where it loses its sensible energy and is stored in the cold tank at temperature $T_{hot} - \Delta T$. The transient equations used are listed in Table 1. M_{hot} , T_{hot} , M_{cold} , and T_{cold} are, respectively, the mass and the temperature of the hot tank and the mass and the temperature of the cold tank. \dot{m}_{collec} and \dot{m}_{boiler} are salt mass flowrates in the collector and boiler, respectively.

In Table 1, w_{sunset} is the sun set time in degrees t_{sunset} and $t_{sunrise}$ are solar sunset and sunrise times.

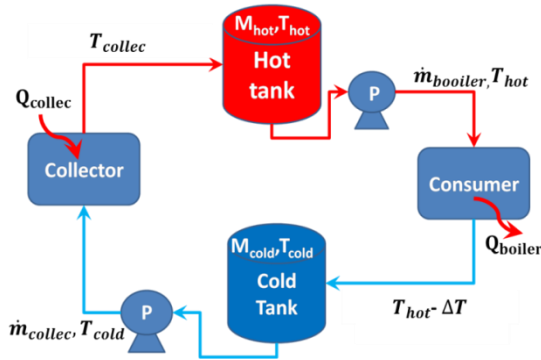


Fig. 2. The heat storage system used in the model.

Table 2. Experimental data and parameters used in the model

Parameter	Value
Heat collection and storage	
Storage time (hr)	15
Collector temperature (°C)	460
Temperature drop over boiler (°C)	275
Rankine reheat cycle	
Upper pressure (bar)	60
Lower pressure (bar)	0.1
Fresh water heater pressure (bar)	6
Turbine inlet temperature (°C)	450
Isentropic turbine efficiency	0.8
Isentropic pump efficiency	0.8
Mass flowrate of water (Kg/hr)	57.8

2.4. Coupling of the three models

From the solar heat collection model the boiler duty and collector heat ($Q_{boilers}$, $Q_{collector}$) are calculated and used in the power plant and the energy storage models, respectively. Consequently, the dynamic response of the system in the form of tank mass, tank temperature, and collector and boiler flowrates are calculated. Fig.3 shows schematically how the three models communicate.

It is assumed that the power plant model responses are much faster than the responses in the heat storage model. Therefore, the power plant model equations are solved under steady state conditions, while those in the heat storage and solar irradiance models are variable with time [1].

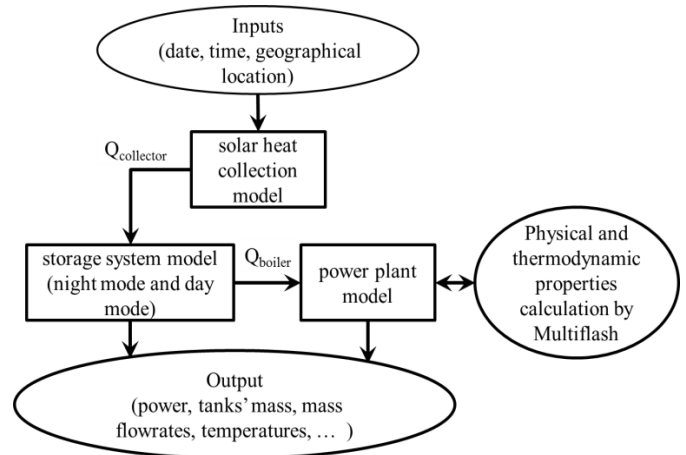


Fig. 3. Structure and communication between the models in CSP model

2.5 Variations of solar irradiance during the day and year

As a case study, our experimental data are the solar radiation data obtained from a weather station, during 10 years in the city of Isfahan, Iran. Isfahan is a city with a relatively high mean irradiance and the results of using solar energy for this area can be utilized as a pattern for other hot cities in the world. However, the data provided during a day are in the form of total collected solar energy and number of sunny hours. To be able to compare the results from the Bird's model (solar irradiance) with those resulting from the experimental data, the methodology in [7] is used and the results are presented in Fig. 4.

Model results and normalized experimental data about the dynamic nature of solar irradiance during a day (May 23rd, as an example) are compared in the figure. The intensity increases from 430 W/m² at 8 am to a maximum of 870 at 12 noon and it decreases again to 430 W/m² during the evening. There is a good agreement between the results with a maximum error of 12%. Similar results were obtained for other days of the year.

Fig.5 shows intensity variations during the year at four solar hours: 9 a.m., 10 a.m., 12 noon, and 2 p.m.. At 12 noon, for example, the intensity increases from 400 W/m² to 800 W/m² by moving from winter to summer. Similar trend, with smaller intensities exist at other hours of the day.

2.6 Calculation of physical and thermodynamic properties

Multiflash is physical and thermodynamic property calculation software. A Multiflash file with water as the only component is defined and different thermodynamic and physical property models are selected in the vapor and liquid phases according to Table 3.

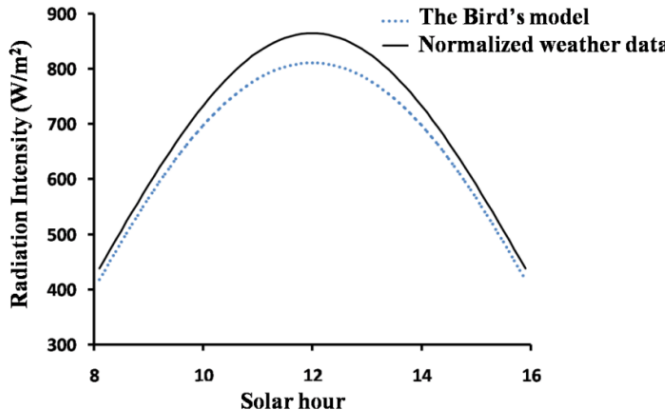


Fig. 4. Comparison of radiation model based on Bird's model with the experimental data (date: May 23, geographic location: (32°37'4" N, 51°39'44"E).

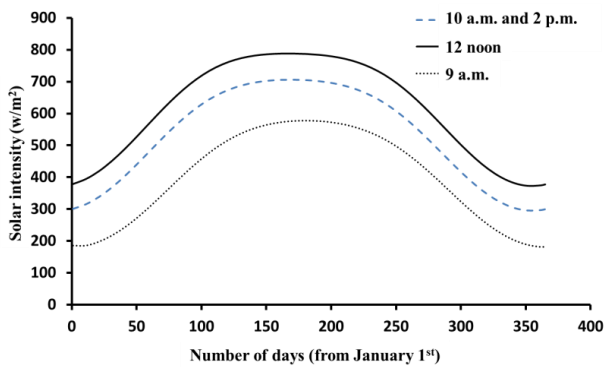


Fig. 5. variations of solar irradiance during the year at 9 am, 10 am, 12 noon, and 2 pm.

3. Results and Discussion

1.1 Power generation during 24 hr

The designed generated power of the power plant is 10 KW. However, it is not necessary to generate electricity during off peak hours. A pattern of charge, according to the electricity consumption of an administration unit, is assumed. Consequently, less power is needed during midnight and the power plant works at the maximum load when needed. The maximum power need is assumed to be between 7:30 am and 4:30 pm. Between 10 ppm and 7:30 am there is a minimum need of 3 KW. The details are shown in Fig.6.

3.2 Tank flow rates and mass flowrates variations during day and night

The mass flowrate of salt melt during the day, from 7:30 am to 16:30 pm, in the collector receiver and in the boiler are shown in Fig.7. The flowrate in the collector increases from the morning to noon, because of increasing solar irradiance. It

increases from 0.025 kg/s at 7:30 am to a maximum of 0.25 at 12 noon and again it decreases to 0.025 kg/s at 16:30. The mass flow rate in the collector is greater than that in the boiler between 9 am and 3 pm, implying the accumulation of solar heat during these hours.

The mass of salt melt in the hot and cold tanks are shown in Fig.8. During the day, hot tank level increases from its min to about 2500 Kg, while in the cold tank, it decreases from a maximum of 2500 Kg to its minimum.

3.3 Importance of heat storage

Heat storage system has two important roles. Firstly, it damps the fluctuatin resulting from variable solar irradiance. Secondly it stors energy for the operation of the plant, during night time and during cloudy hours. To calculate these effects, imagine the CSP plant in the absence the two storage tanks. The collector heat is simultaneously transferred to the boiler:

$$Q_{\text{collector}} = Q_{\text{boiler}} \tag{26}$$

Table 3. Correlations used to calculate thermodynamic and physical properties of pure components

PARAMETER	EQUATION
Equation of state	$P = \frac{NRT}{V - b} + \frac{a}{V^2 + 2bV - b^2}$
Specific heat	$\frac{c_P}{R} = a_3 + (a_4 - a_3)y^2(1 + (y - 1)F(y))$
Density	$\rho = \frac{1}{V_c} + a_1\tau^{1/3} + a_2\tau^{2/3} + a_3\tau + a_4\tau^{4/3}$
Thermal conductivity	$\lambda = a_1(1 + a_2\tau^{1/3} + a_3\tau^{2/3} + a_3\tau)$

Therefore, the required surface area to reach to the same boiler capacity, considering the changes in solar irradiance during a day, can be obtained. The results are shown in Fig.9. In the absence of storage system, at the early mornings, more than 1500 m² surface area is necessary and near the noon this surface reduces to only 100 m². In other words, by applying a surface area of 350 m² and suitable design of storage tanks, we have prevented these extreme requirement limits in the surface area. Furthermore, the operation of the power plant during the night has become possible.

The importance of storage system can be shown, also, by assuming a fixed surface area and calculating the "imaginary"

outlet temperature from the boiler. The results indicate that at surface area ranges of 100 m² to 300 m², a boiler steam temperature is greater than 1000 °C during noon. Design, operation, and safety of the equipment to afford this high temperature are not possible in practice. These results clearly indicate that storage tanks are one of the unavoidable parts for the operation of CSP plants.

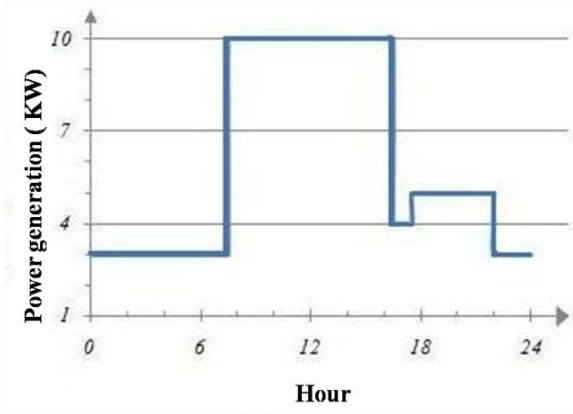


Fig. 6. Power generation during day and night.

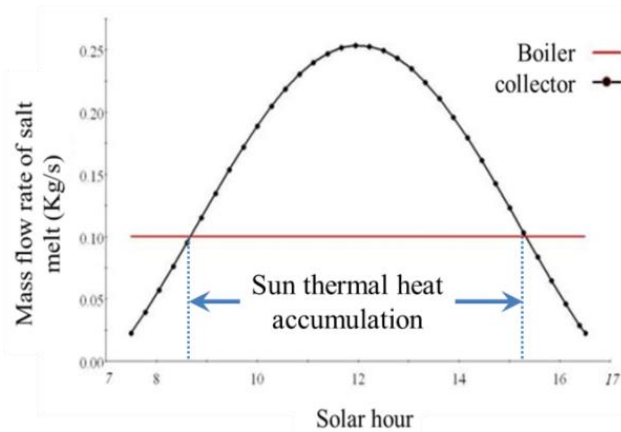


Fig. 7. Mass flow rates of salt melt in the boiler and collector.

4. Conclusion

A flexible gPROMS model for CSP plants with heat storage is developed. Based on the calculations made for the shortest day of the year, when the solar irradiance changes from around 300 W/m² to 800 W/m², the instantaneous mass flow rates of heat transfer fluid through solar collector receiver and through boiler change between 0.025 Kg/s and 0.25 Kg/s. Assuming a pattern of electricity consumption similar to that of an administration unit with a maximum electricity need of 10KW, a total mass of 2500 Kg of heat transfer fluid and storage medium is required. Without storage tanks, the

amount of fluctuations in the temperature or the required surface area of collector are huge. The results predict either variable surface area between 100 m² and 1500 m² or vary high boiler temperatures of 1000 °C which avoids the plant operation in practice.

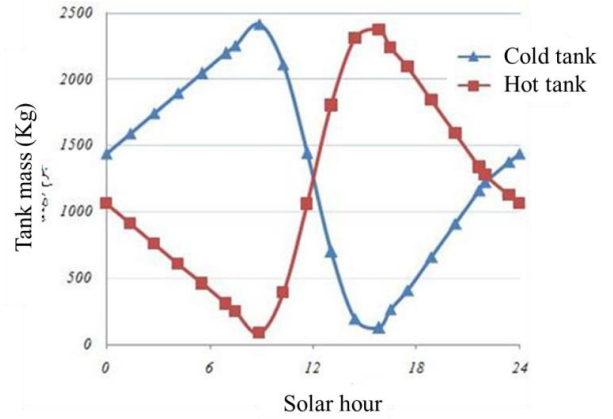


Fig. 8. Variations in the hot and cold tanks' masses during day and night

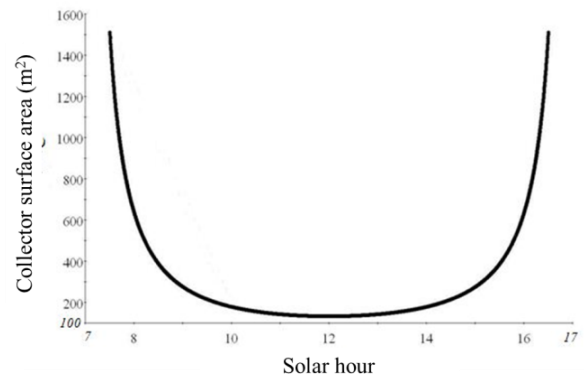


Fig. 9. Required surface area of collector in the absence of storage tanks

Acknowledgements

The authors acknowledge the financial support received from the dean of research at the University of Isfahan.

References

[1] S.F. Hosseini, B.M. Goortani, M. Niroomand, Instantaneous Responses of on-grid PV Plants to Changes in Environmental and Weather Conditions, *International Journal of Renewable Energy Research*, (2016) 6(4) (in press).
 [2] J.D.Osorio, R. Hovsapijan, J.C.Ordenez, Dynamic analysis of concentrated solar supercritical CO₂-based power

generation closed-loop cycle, *Applied Thermal Engineering*, (2016) 93(25), 920–934.

[3] B.M. Goortani, A. Gaurav, A. Deshpande, F.T.T. Ng, and G. L. Rempel, Production of Isooctane from Isobutene: Energy Integration and Carbon Dioxide Abatement via Catalytic Distillation, *Industrial Engineering and Applied Chemical Research*, (2015) 54 (14), 3570–3581.

[4] A.Gil, M.Medrano, I.Martorell, A.Lázaro, P.Dolado, B.Zalba, L.F.Cabeza, State of the art on high-temperature thermal energy storage for power generation: Part 2—Case studies, *Renewable and Sustainable Energy Reviews*, (2010) (14) 56-72

[5] R.E.Bird, R.L.Hustrom, A simplified clear sky model for direct and diffuse insolation on horizontal surface, *Solar Energy Research Institute*, SERI/TR-642-761 (1981).

[6] Duffie, J.A., Beckman, W.A., Solar engineering of thermal processes, 2ND ed., John Wiley & Sons Inc. (1980).

[7] A. R. M. Collares-Pereria, The average Distribution of Solar Radiation- Correlations between Diffuse and Hemispherical and between Daily and Hourly Insolation Values, *Solar Energy*, (1979) (22).

[8] R.E.Sonntag, C.Borgnakke, G.J. Van Wylen, Fundamentals of Thermodynamics, Mc GraHill Publications, 6th ed. (2003).

[9] L.Y. Bronicki, History of Organic Rankine Cycle systems, Organic Rankine Cycle (ORC), Power Systems, (2017) 25-66.

[10] B.M. Goortani, E. Mateos Espejel, J. Paris, Integration of a cogeneration unit into a Kraft pulping process, *Applied Thermal Engineering* (2010) 30, 2724-2729.

[11] I.L. Garcá, J. Luis, D. Blanco, Performance model for parabolic trough solar thermal power plants with thermal storage: Comparison to operating plant data, *Solar Energy*, (2011) 85(10) 2443–2460

[12] S. Suojanen, E. Hakkarainen, M. Tähtinen, T. Sihvonen, Modeling and analysis of process configurations for hybrid concentrated, solar power and conventional steam power plants, *Energy Conversion and Management*, 134 (2017) 327–339.

[13] N. Lorenzin, A. Abanades, A review on the application of liquid metals as heat transfer fluid in Concentrated Solar Power technologies, *International Journal of Hydrogen Energy*, 41(2016) 6990-6995.

[14] S.Ravelli, G.Franchini, A.Perdichizzi, S.Rinaldi, V.E. Valcarenghi, Modeling of Direct Steam Generation in Concentrating Solar Power Plants, *Energy Procedia* 101 (2016) 464– 471.

[15] Y. Jian, F. Bai, Q. Falcoz, Z. Wang Control Strategy of the Module Concrete Thermal Energy Storage for parabolic Trough Power Plants, *Energy Procedia*, 69 (2015), 891-899.

Nomenclature

$Area$	solar collector area (m ²)
C_p	heat capacity (J/Kg.°C)
FWH	fresh water heater
G_{cb}	clear-sky horizontal beam radiation
G_{on}	extraterrestrial radiation incident on the plane normal to the radiation
G_{sc}	solar constant 1367 w/m ²
h	molar enthalpy (J/mol)
I_0	solar intensity (W/m ²)
I_b	solar intensity, Bird's model (W/m ²)
L	liquid molar flow rate (mole/s)
M	mass (kg)
\dot{m}	mass flow rate (kg/s)
P	Pressure
Q_c	condenser load (kW)
T	Temperature
T_{h1}	inlet hot fluid temperature (K)
T_{h2}	outlet hot fluid temperature (K)
T_{c1}	inlet cold fluid temperature (K)
T_{c2}	outlet cold fluid temperature (K)
T_b	atmospheric transmittance for beam radiation
ϵ	Effectiveness
γ	vapor quality
W_{sunset}	sunset angle hour
δ	declination angle
ϕ	Latitude
η	Efficiency
ρ	density (Kg/m ³)
λ	thermal conductivity W/(m. K)
Subscripts	
in	inlet stream
out	outlet stream
gen	Generator
T	Turbine
$cond$	condenser
hot	hot tank
$cold$	cold tank